



Cell-free immunomodulatory biomaterials mediated *in situ* periodontal multi-tissue regeneration and their immunopathophysiological processes



Guanqi Liu^{a,b,1}, Xuan Zhou^{a,b,1}, Linjun Zhang^{a,b,1}, Yang Zou^{a,b}, Junlong Xue^{a,b}, Ruidi Xia^{a,b}, Nuerbiya Abuduxiku^c, Xuejing Gan^{a,b}, Runheng Liu^{a,b}, Zhuofan Chen^{a,***}, Yang Cao^{a,**}, Zetao Chen^{a,b,*}

^a Hospital of Stomatology, Guanghua School of Stomatology, Sun Yat-sen University, and Guangdong Provincial Key Laboratory of Stomatology, Guangzhou, 510055, China

^b Guangdong Research Center for Dental and Cranial Rehabilitation and Material Engineering, Guangzhou, 510055, China

^c Department of Stomatology, Kashgar First People's Hospital, Kashgar, Xinjiang, 844000, China

ARTICLE INFO

Keywords:

Biomaterials
Immunopathophysiological processes
Endogenous regeneration
Periodontal multi-tissue regeneration

ABSTRACT

Cell-free biomaterials-inducing endogenous *in situ* multi-tissue regeneration is very challenging and applying advanced immunomodulatory biomaterials can be an effective strategy to overcome it. In-depth knowledge of the immunopathophysiological mechanisms should be acquired before applying such an immunomodulation strategy. In this study, we implanted different immunoregulatory cell-free biomaterials into periodontal multi-tissue defects and showed that the outcome of multi-tissue regeneration is closely regulated by the immune reaction. The underlying immunopathophysiological processes, including the blood clotting response and fibrinoid necrosis, innate and adaptive immune response, local and systemic immune reaction, growth factors release, and stem cells recruitment, were revealed. The implantation of biomaterials with anti-inflammatory properties could direct the immunopathophysiological process and make it more favorable for *in situ* multi-tissue regeneration, ultimately enabling the regeneration of the periodontal ligament, the acellular cementum matrix, and the alveolar bone in the periodontium. These findings further confirm the effectiveness of immunomodulatory based strategy and the unveiling of their immunopathophysiological processes could provide some favorable theoretical bases for the development of advanced cell-free immunomodulatory multi-tissue regenerative biomaterials.

1. Introduction

Tissue regeneration involves the repair and functional integration of multiple different structures. For example, the human periodontium consists of interconnected structures of soft and mineralized tissues, including the periodontal ligament, cementum and alveolar bone [1]. The regeneration of periodontium requires the deposition of the new cementum of the root surface, restoration of the alveolar bone, the regeneration of the functionally oriented periodontal ligament fibers. It is very challenging to achieve the regeneration of a multi-tissue, such as the periodontium. A scaffold containing tissue-derived primary cells has been developed to promote multi-tissue regeneration [2]. Although

promising preliminary results were achieved in these studies, the technique of combining exogenous stem cells with elaborately synthetic biomaterial scaffolds is intricate [3].

Endogenous *in situ* regeneration aims to recruit adult stem cells from specialized “stem cell niches” present in a multitude of tissue/organs to the injury site for them to differentiate into different cell types, ensuring multi-tissue regeneration [4,5]. The purpose of this technology is to provide a new strategy for utilizing the biological resources of a given body and their reparative capability for multi-tissue regeneration, especially at sites with cells from diverse sources and a complex tissue structure [6]. Endogenous *in situ* regeneration may become an effective strategy to achieve multi-tissue regeneration.

* Corresponding author. Hospital of Stomatology, Guanghua School of Stomatology, Sun Yat-sen University, and Guangdong Provincial Key Laboratory of Stomatology, Guangzhou, 510055, China.

** Corresponding author.

*** Corresponding author.

E-mail addresses: chzhuof@mail.sysu.edu.cn (Z. Chen), caoyang@mail.sysu.edu.cn (Y. Cao), chenzet3@mail.sysu.edu.cn (Z. Chen).

¹ These authors contributed equally to this work.

However, the homing and functioning of stem cells are controlled by the coordinated interactions of a vast network of chemokines, cytokines, growth factors, and adhesion molecules [7,8]. The spatial and temporal release and the interactions of these factors are dominated by the immune microenvironment [9]. The outcome of tissue regeneration, including the healing process and the type of regenerated tissue, is influenced by the immune response [10]. The development of cell-free biomaterials to direct the immune response towards a scenario that is favorable for *in situ* multi-tissue regeneration is becoming attractive [11].

Directing the immune regulation for *in situ* multi-tissue regeneration is difficult. Some *in vitro* studies have shown that the proinflammatory microenvironment is responsible for debridement, whereas the anti-inflammatory microenvironment is vital for tissue regeneration [12–14]. However, the *in vivo* context is more complicated, especially for the achievement of multi-tissue regeneration, which requires the collaboration of multiple immune biomolecules that are released from different immune cells belonging to different immune systems [15,16]. This immunopathophysiological process, which includes the coordinated interactions among immune cells, stem cells, cytokines, growth factors, navigational cues, and even the immune response in remote organs, is complex [17,18].

Due to this complex immune environment-mediated multi-tissue regeneration, it is of great importance to understand how the implanted immunomodulatory multi-tissue regenerative biomaterials affect this immunopathophysiological process *in vivo* and the subsequent effects on *in situ* multi-tissue regeneration. In this way, a more sophisticated knowledge of the evolution of this process could be developed and enlighten the development of effective multi-tissue regeneration approaches.

LPS and IFN γ has been regarded as effective proinflammatory factors for inducing the transformation of the M1 type macrophages or CD4⁺ T helper 1 cells and tending to cause the apoptosis of MSCs, foreign body reaction and the chronic inflammation. Whereas, IL4 is a typical anti-inflammatory factor with the ability to induce the activation of M2 type macrophages or CD4⁺ T helper 2 cells and is often associated with the proliferation and differentiation of tissue-resident progenitor cells, fibrillogenesis and tissue healing. Periodontium is a typical multi-tissue defect model, requiring the restoration of cementum deposition on the root surface, the formation of interconnected periodontal ligament fibers, and the restoration of alveolar bone [1]. Nowadays, the most common strategy used for clinically regenerating the periodontium is the implantation of a biological hydroxyapatite-like material, such as Bio-oss® [19]. While this strategy has achieved certain clinical success in regenerating bone tissue, the complete regeneration of the cementum-periodontal ligament-bone complex is still challenging [20]. In this study, we primarily used the biogenic hydroxyapatite as a model material and adopted with LPS/IFN γ and IL4 respectively to form immunoregulation biomaterials. We then implanted different immunoregulatory cell-free biomaterials into periodontal multi-tissue defects in rats, attempting to unveil its immunopathophysiological process, and their eventual effects on the *in situ* periodontal multi-tissue regeneration outcomes. Here we have mapped the immunopathophysiological profiles for periodontal multi-tissue regeneration triggered by different immunoregulation biomaterials *via* integrating a complex set of biological events of the acute injury histological reaction, phenotype transition of innate immune cell subsets, interaction networks of immune cytokines, expression of growth factors and the recruitment of stem cells as well as the involvement of systemic immune reaction from acute reactive phase to tissue remodeling stage. This study can provide some favorable theoretical bases for the development of advanced cell-free immunomodulatory multi-tissue regenerative biomaterials that can better mimic the *in vivo* scenario, bearing in mind the immunopathophysiology.

2. Results and discussion

2.1. Successful preparation of the materials and the periodontal multi-tissue defect model

Porcine hydroxyapatite (PHA) was applied as a scaffold material to construct immunomodulatory cell-free biomaterials. PHA was prepared from cancellous porcine bone, which is similar to human bone in terms of the macrostructure, microstructure, bone composition and bone remodeling properties [21]. Further, polydopamine (PDA) coating was formed on the surface of PHA *via* simply immersing PHA in alkaline dopamine solution. With much reactive functional groups like amine and catechol content, the surface modification of PDA could immobilize immunomodulatory factors LPS/IFN γ and IL4 *via* mechanical adsorption, Schiff base reaction or Michael addition reactions [22,23] (Fig. 1A). Particles smaller than 0.2 mm could induce strong foreign body reaction, which may cause poor regeneration effect [24,25]. As the size of the rat periodontal defect in this study was 5*2*1 mm, PHA particles smaller than 0.5 mm can achieve better maintenance after implanting into the defect. Therefore, in this study the size distribution of PHA particle was 0.2–0.5 mm (Table 1), which is suitable to be used in rat periodontal defect and will not elicit strong proinflammatory response. After PDA coating, the color was changed to gray while no morphology and crystal structure change was confirmed by SEM and XRD result (Fig. 1B and C). The XPS result suggest the presence of Ca, P, O element in PHA. For PDA-PHA the characteristic N element was measured (Fig. 1D). As suggested by FTIR result, the absorption peak at the 1618 cm⁻¹ is identified as the characteristic absorption band of benzene ring and was also shown at PDA and PDA-PHA group (Fig. 1E). These results confirmed the successful construction of PDA coating on the surface of PHA. The ELISA results further demonstrated the decrease in the IL4 and IFN γ levels in the soaking medium, indicating an increased adsorption on the surface of PDA-PHA (Fig. 1F). Each milligram of PHA could adsorb approximately 30 EU of LPS (Fig. 1G). The immunofluorescence staining was performed to visualize the distribution of LPS/IFN γ and IL4 on the PDA-PHA surface (Fig. 1H). These results collectively demonstrate the successful loading of LPS/IFN γ and IL4 on the PDA-PHA surface.

A critical-size rat periodontal defect model was then prepared (Fig. S1A). The 5 × 2 × 1 mm size could avoid self-healing during the observation period according to previous researches [26,27]. Besides, according to the anatomical structure of the rat maxillofacial region, with the depth of 1 mm, the periodontal multi-tissue defect, including the defect of cementum-periodontal ligament-alveolar bone structure could be achieved (Fig. S1B). PDA-PHA (control group), LPS/IFN γ -PDA-PHA (LPS group), and IL4-PDA-PHA (IL4 group) were respectively implanted into this periodontal multi-tissue defect model to achieve the complex regeneration and to unveil their immunopathophysiological processes.

2.2. Immunomodulatory biomaterials regulate the local immunopathophysiological process

Generally, implanted biomaterials can modulate the blood clot response by releasing a number of immune cell chemokines [28]. Innate immune cells are recruited to the lesion, where they regulate the local immune microenvironment and degrade the biomaterials [29]. The immune system may be stimulated with antigen presentation. Activated adaptive immune cells could migrate to the lesion, participating in the modelling of the local immune environment [30]. With the release of cytokines from immune cells, progenitor or stem cells from the periodontal ligament and alveolar bone marrow can be recruited, initiating the neo-tissue regeneration and the tissue remodeling stage [31]. Therefore, the effects of different immunoregulatory PHA materials on

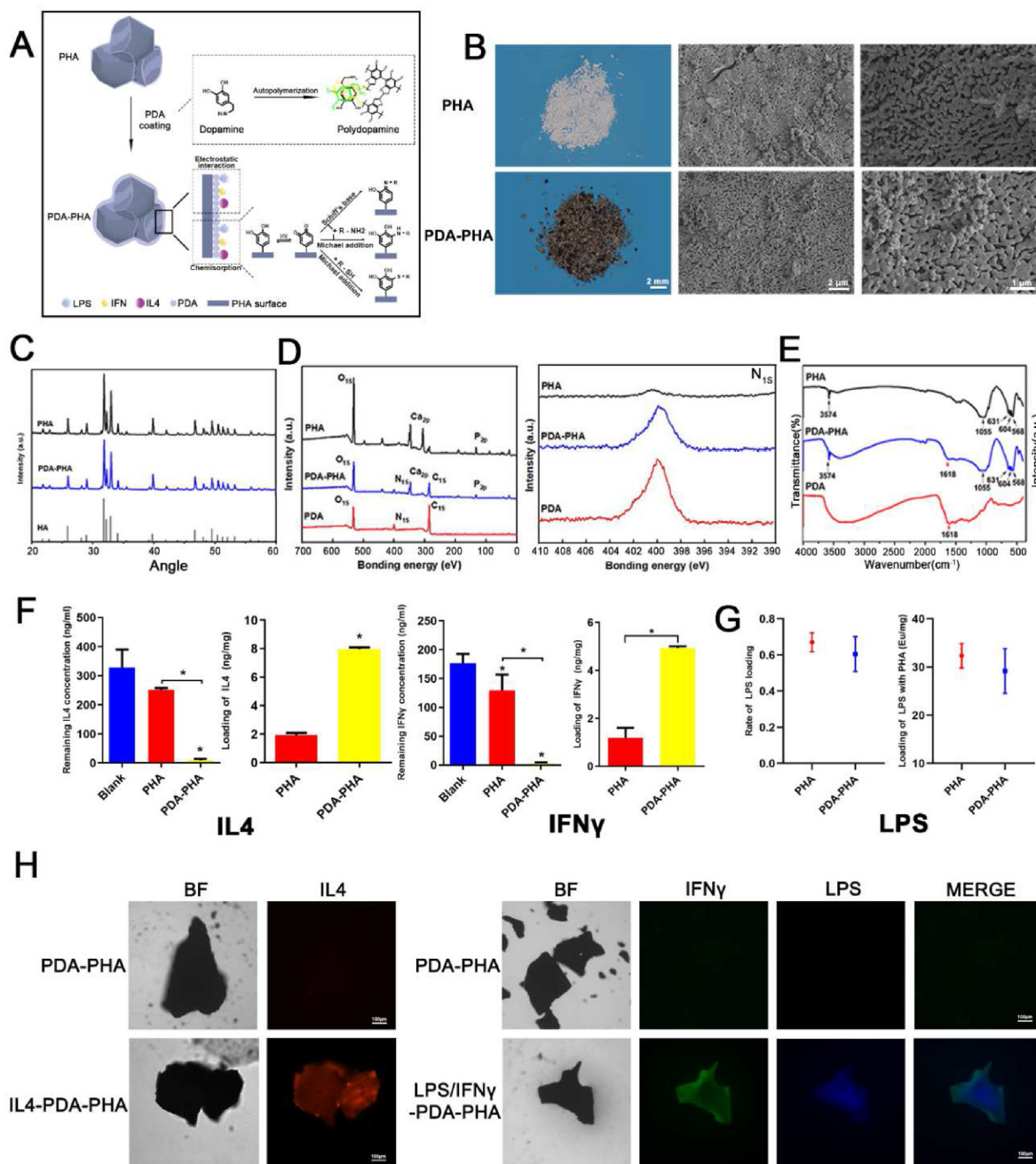


Fig. 1. Preparation and characterization of the biomaterials. A) Schematic figure of the mechanism of PDA coating formation and the immobilization of immune regulatory factors. B) Macroscopic images of PHA and PDA-PHA show the color of PDA-PHA turn gray, while the SEM image shows no obvious morphology differences; C) The XRD results showed no crystal structure changes in PDA-PHA; D) The XPS results confirmed the N1s peak in PDA-PHA; E) The FTIR results showed the benzene ring in PDA-PHA. F) The ELISA results show the decrease of IL4 and IFN γ in the solution after soaking the PDA-PHA particles, which indicated the loading of IL4 and IFN γ on the PDA-PHA respectively; G) The decrease of LPS in the solution after soaking PHA or PDA-PHA; H) The immunofluorescence staining shows the loading of IL4 and LPS/IFN γ on the surface of PDA-PHA particles respectively. (* PHA vs. PDA-PHA, $p < 0.05$).

inducing different local immunopathophysiological processes were further investigated.

2.2.1. Acute injury reactions and the initiation of multi-tissue repair process

After material implantation for 3 days, an acute injury reaction with the formation of blood clot fibrin entrapping materials could be observed. A few mononucleated cells could be found on the surface of the materials (Fig. 2A). In the LPS group, the blood clot fibrins were thick and formed a sparse network (Fig. 2A, Fig. S3). It provided a provisional protection for the denuded tissues especially on the surface of dentin and alveolar bone. On the other hand, this implied the precipitation of fibrin,

which has been found to be negatively related with the periodontal tissue regeneration but favorable for immune cell activation [32]. Moreover, we found severe fibrinoid necrosis of the periodontal ligament tissue at the edge of the defect (Fig. 2A blue box). The fibrinoid necrosis formed as a barrier between the defect and remaining tissue, preventing the further invasion of exogenous substance. It could be regarded as a self-protection mechanism of organism and showed positive correlation with the degree of the local damage [15]. However, this fibrinoid necrosis barrier may also block the transport of stem cells, immune cells, nutrients and extracellular matrix (ECM) molecules from periodontal ligament and negatively affected the process of tissue repair as no apparent periodontal

Table 1
The maximum and minimum Feret diameter of the PHA particles.

Number	maximum Feret diameter ^a (μm)	minimum Feret diameter ^b (μm)
1	431.496	304.806
2	265.286	222.843
3	450.005	234.823
4	444.285	309.261
5	428.964	356.582
6	296.240	227.341
7	416.468	295.577
8	345.116	265.777
9	337.062	262.019
10	426.541	295.875

^a Maximum Feret diameter represents the longest dimension of the particle independent of its angular rotation at the time the image was captured. The maximum Feret diameter is determined by isolating the corner pixels of the object's perimeter and taking the maximum distance between each corner pixel to all other corner pixels.

^b The minimum Feret diameter is defined as closest possible distance between the two parallel tangents of an object.

multi-tissue regeneration signs were observed. Together, these results indicate that the LPS group may have had an enhanced acute injury inflammation, thus causing severer local tissue damage with a set of self-protection measures to protect the remaining tissues from further invasion. Meanwhile, this over defensive action may also result in a restraint to tissue regeneration.

Interestingly, this self-protection mechanism seemed to fade away and the tissue regeneration process seemed to begin on day 7. The thick fibrin network began to be degraded and became thinner (Fig. 2B). Multinuclear giant cells (MNGCs) could be observed at the edge of the periodontal ligament defect (Fig. 2B blue box), degrading the fibrinoid necrosis, and the periodontal ligament began to be in contact with the fibrin network in the lesion, leading to the generation of rare periodontal collagen fiber [33]. Stem cell homing is an important strategy in the development of biomaterials-based endogenous *in situ* multi-tissue regeneration. Thus, the recruitment of stem cells was further evaluated in this stage. CXCL12 is a stem cell homing factor that binds to the CXCR4 receptor and plays a role in the recruitment, migration and differentiation of stem cells [34,35]. It has been demonstrated that CXCR4⁺ MSCs can be recruited to the injury site *via* chemotactic attraction toward a gradient of CXCL12 [36]. The expression of CXCL12 in LPS group did not markedly increase at day 3 but was slightly upregulated at day 7 (Fig. 2C). However, the recruitment of stem cells that are positive for the mesenchymal marker CD90 and negative for the hematopoietic marker CD34 was not evident (Fig. 2D). These results imply that the enhanced acute injury inflammation was being resolved and that the host body was going to initiate the repair process but only in its preparatory phase as the recruitment of stem cells was not obvious.

However, the results obtained for the IL4 group were different from that of the LPS group. At day 3, the generation of periodontal ligament fibrinoid necrosis was inconspicuous (Fig. 2A). The blood clot fibrins were thin in diameter but luxuriant, velvety, and connected *via* a dense network, which can provide conditions for cell migration and substance exchange, creating the foundation for further regeneration [37]. Compared with LPS group, these results point to the fact that IL4 could reduce acute injury inflammation, while initiating multi-tissue repair.

With this favorable environment, a multi-tissue regeneration process could be observed at day 7. MNGCs were rarely found at the defect edge of the periodontal ligament, but were observed surrounding the implanted materials, indicating the beginning of material degradation (Fig. 2B). Moreover, with the up-expression of CXCL12 at day 3 and 7, the IL4 group exhibited stronger stem cells homing ability (Fig. 2C). The obvious recruitment of CD90⁺ CD34⁻ stem cells to the defect site was observed (Fig. 2D). The signs of the periodontal bone-ligament-cementum complex regeneration emerged. The network of blood clot

fibrin was gradually replaced by the newly formed collagen fibers, which could be further mineralized to form bone tissue [38]. Regarding the cementum-periodontal ligament regeneration, functional ALP positive fibroblasts were observed on the surface of the denuded dentin (Fig. 2E), which has been known to secrete a collagen bundle vertical to the tooth root surface (namely, Sharpey's fibers) and is a resource of acellular cementum matrix [39–41]. Therefore, these results indicate the onset of this complicate multi-tissue repair process in the IL4 group, characterized by the formation of the periodontal structure (Sharpey's fibers) and the potential formation of acellular cementum and bone tissue.

From our results, it could be speculated that the proinflammatory effect in the LPS group may cause more severer damage to the local tissue thereby inducing intense defensive reactions such as severe fibrinoid necrosis and thicker blood clot fibrin to protect the remaining tissue from further invasion. However, this over defensive action may against the process of tissue regeneration. While anti-inflammatory effect of IL4 may reduce the damage to the tissue to avoid over defensive reaction, providing conditions for cell migration and substances exchange, founding basis for further regeneration process.

2.2.2. Characterization of the generated immune microenvironments

Typical immune regulators, the immune regulation effect of which has been widely known and commonly used in evaluating the general characteristics of the immune microenvironment, were further analyzed (Fig. 3A and B). In order to get a general overview of these cytokines including their general correlation and the differentially expression distribution among different groups, the cytokines networks in Fig. 3B and D were performed to show the interaction of the cytokines. These cytokines were classified with their most widely recognized immune regulation properties and marked with different color for the up-regulation cytokines in each group (yellow for those upregulated in control group, red for those regulated in LPS group and green for those upregulated in IL4 group) to map the immune cytokines functional profile of different groups. TNF α , IFN γ , and NF- κ B (RelA) have been known as typical pro-inflammatory factors and trigger the local inflammatory response [9, 18]. At day 3, in LPS group, the proinflammatory response featured as the upregulation of the TNF α , IFN γ , and NF- κ B (RelA) levels. The upregulation of the expression levels of the M1 macrophage markers (CD86 and CCR7) and the Th1 marker (Tbx21) could also be observed. Th1 chemokines CCL17 and CXCR3 were both upregulated. These results collectively indicate the possible involvement of Th1 and M1 macrophages. The results of the IHC analysis further confirmed this hypothesis. The amount of M1 macrophages in the LPS group was markedly higher than that of the other groups (Figs. 4A and S4). This result was also confirmed by immunofluorescent staining in Fig. S5. Interestingly, in addition to this Th1-M1 interaction, B cell chemotaxis which can be induced by CXCR5 [42] was also upregulated in LPS group (Fig. 3B), which implied the possible recruitment of B cells and the complexity of this immunopathophysiological process. These results implied a type 1 immune response-dominated pro-inflammatory immune environment in LPS group.

However, at day 7, the gene expression profile of the immune factors was markedly changed in the LPS group (Fig. 3C and D). Pro-inflammatory cytokines were down-regulated, while the upregulation of immune regulatory cytokines, including TGF β 1 and TGF β 3 both of which often regarded as anti-inflammatory factors, could be observed. CD68, CD11b (Itgam) and CD45 (Ptprc) have been regarded as pan-macrophage markers and CD163 has been reported as the M2 macrophage marker [9]. The expression of CD68, CD11b (Itgam), CD45 (Ptprc) and CD163 were upregulated. The number of CCR7 positive macrophages was still the highest in the LPS group (Fig. 4B and S4). Though the number of CD206 positive cells was still the lowest, the growth rate of CD206 positive cells was the highest in the LPS group (Fig. 4C). MNGCs characterized as TRAP and CCR7 positive were generated and were mainly distributed in the

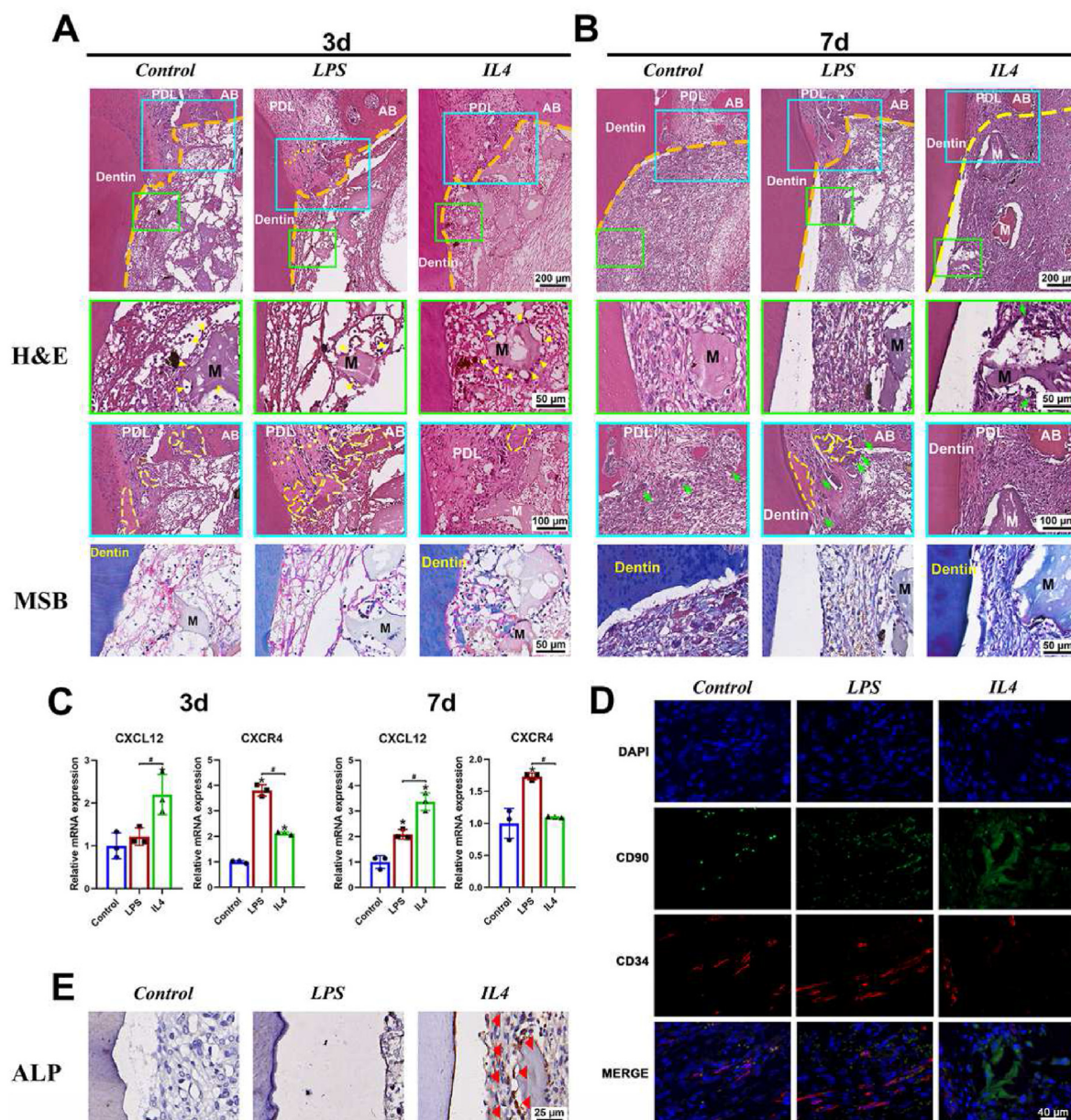


Fig. 2. The acute injury reaction and initial multi-tissue repair process after implanting the immunomodulatory biomaterials. A-B) H&E and MSB staining of the defect area at day 3 and 7. A) At day 3, blood clot fibrins with different morphology were formed. (green box). Mononucleated cells could be found on the surface of the materials (yellow arrow head). A severe acute injured reaction with a thick blood clot fibrin network and periodontal ligament fibrinoid necrosis (yellow dotted line) was found in the LPS group, whereas it was inconspicuous in the IL4 group (blue box). In MSB staining, blood clot fibrin appears in red, while the collagen fibers appear in blue. B) At day 7, the network of blood clot fibrin was gradually replaced by the new-formed collagen fibers to varying degrees among all the groups (green box). The thick fibrin began to be degraded and MNGCs (green arrow) could be observed at the edge of the defect in the LPS group. In the IL4 group, the boundary of newly formed collagen and the remaining periodontal ligament was obscure (blue box). MSB staining shows the blood clot was gradually replaced by collagen fiber on day 7. C) Gene expression level of CXCL12 and CXCR4 at day 3 and 7. D) Immunofluorescence staining of CD90 (green) and CD34 (red) at day 7. E) ALP staining of the local area at day 7. ALP positive stained cells (red arrow head) could be observed on the surface of the denuded dentin in IL4 group. PDL: periodontal ligament; M: materials; AB: alveolar bone; orange dotted lines: the boundary of the prepared defect. (* control vs. LPS/IL4 group, # LPS vs. IL4 group, $p < 0.05$).

defect edge of the periodontal ligament (Fig. 4D and E), accounting for the degradation of fibrinoid necrosis. All these results show a tendency of a shift from a proinflammatory type 1 immune response towards a wound healing type 2 immune response in the LPS group.

As aforementioned, an anti-inflammatory immune environment was observed at day 3 in the IL4 group (Fig. 3A and B). With the upregulation of the levels of the anti-inflammatory cytokines TGF β 1 and IL13, the M2 macrophages were the dominant immune cells, with an upregulation of Arg, CD163, and CD206 (Mrc1). The IHC results further showed an increased number of CD206 positive macrophages (Fig. 4A). The

upregulation of Th1 chemokines (CCR5, CXCL6, and CXCL9) and Th2 chemokines (CCL7 and CCL2) suggested the possible involvement of T cells.

The inflammatory status at day 7 was not evident (Fig. 3C and D). However, the expression of anti-inflammatory factors and proinflammatory factors decreased in the IL4 group. The Th1 (CXCR3, CXCL10, CXCL9 and CCL17) and Th2 (CCR4, IL5, CCL2) activation related factors were still upregulated (Fig. 3C). The CD206 expression level and the number of CD206 positive macrophages were still the highest in the IL4 group (Fig. 4B, S4 and S5). It was speculated that the

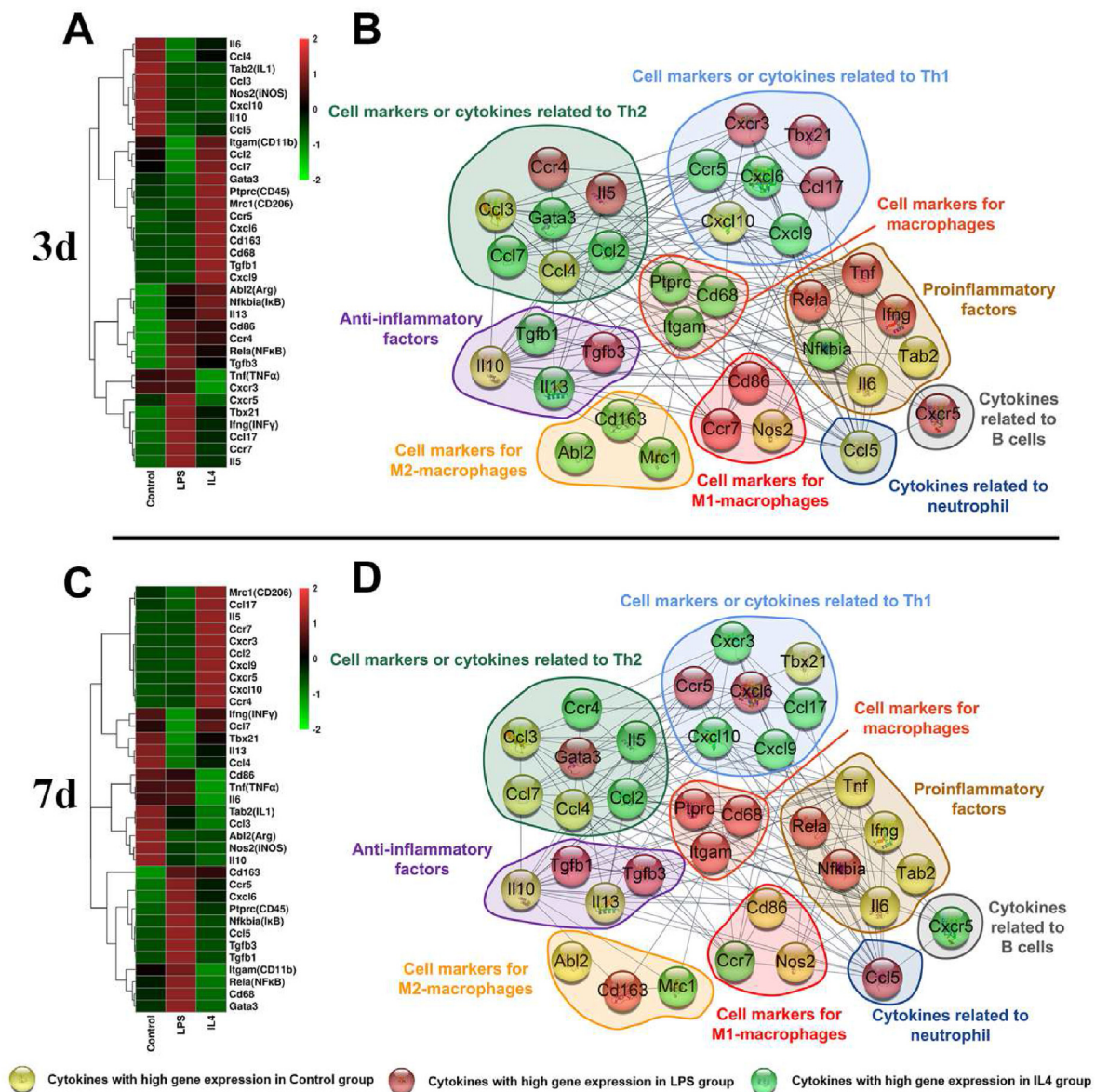


Fig. 3. Gene analysis of the local immune environment at day 3 and 7. A, C) Clustering heatmap shows the differential gene expression of immune cytokines at day 3 and 7. B, D) The functional interaction network shows the characteristics of the local immune microenvironment at day 3 and 7. Cytokines were classified according to their function. The factors with a high expression in the control, LPS, and IL4 groups are marked in yellow, red, and green, respectively.

TRAP and CD206 positive MNGCs were responsible for the material degradation since they were founded nearby the materials (Fig. 4D and E). The role of MNGCs in biomaterials-mediated tissue regeneration remains controversial. Originally MNGCs were considered to be responsible for the tissue degradation and material rejection being referred as foreign body giant cells (FBGCs). In recent researches, MNGCs has been found to secrete anti-inflammatory factors such as IL10, IL13 and TGF β , contributing to tissue regeneration. Different phenotypic profiles of MNGCs have been found [29,43]. The contradictory effect on tissue regeneration may own to their phenotypic heterogeneity. According to our results, MNGCs seem to exhibit a phenotypic heterogeneity which is equivalent to that of macrophages suggesting that MNGCs could play a significant role in tissue regeneration in a manner comparable to macrophages. MNGCs here could be regarded as a “functional syncytium” of macrophages. The CD206 positive MNGCs may attribute to the improved multi-tissue regeneration in IL4 group while the CCR7 positive ones may play more role in absorbing fibrinoid necrosis in LPS group. These results

indicate that in IL4 group immune homeostasis was approaching as the multi-tissue regeneration was in progress.

2.2.3. The effects of generated immune microenvironments on the multi-tissue regeneration regulatory factors

The expression of the regenerative regulatory factors could be regulated by the immune microenvironment. The protein-protein interaction network analysis results showed that the upregulated immune factors in either the LPS or IL4 group are closely related with the regenerative factors (Fig. 5A). The function of these regenerative factors can be classified as fiber remodeling related factors, osteogenic factors, angiogenic factors and cementum mineralization-related factors (Fig. 5B). At day 3, the connecting lines between upregulated immune factors and the regenerative factors in LPS group were marked sparser than that of the IL4 group. Under the proinflammatory environment on day 3 in the LPS group, no remarkable upregulation of multi-tissue regenerative factors was observed (Fig. 5A, C). Regarding day 7, the immune environment

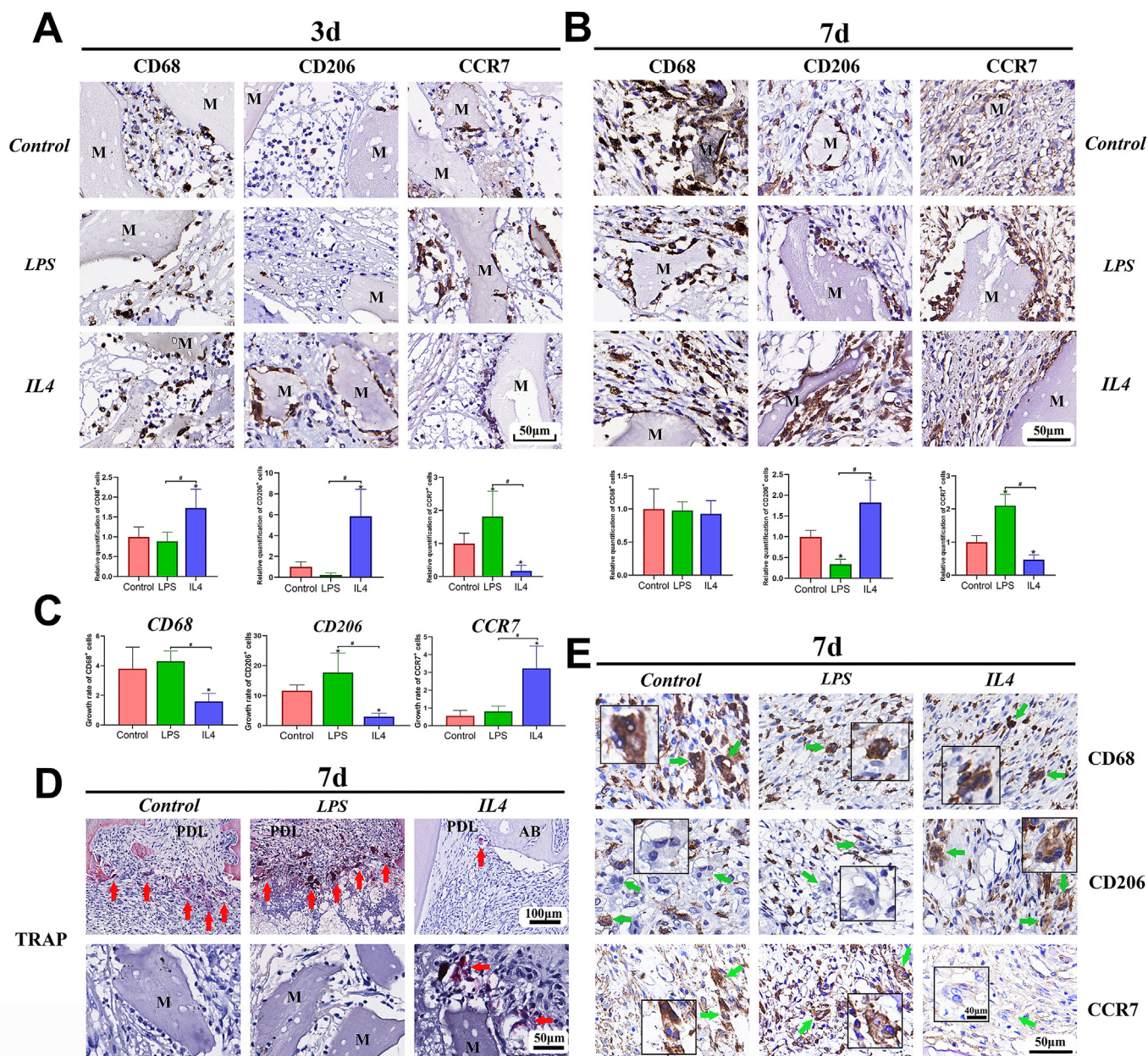


Fig. 4. Histological analysis of the local immune environment at day 3 and 7. A-B) IHC staining image and quantitative analysis of the CD68⁺, CD206⁺, and CCR7⁺ cells at day 3 and 7. C) The growth rate of CD68⁺, CD206⁺, and CCR7⁺ cells from day 3–7. D) MNGCs could be observed via TRAP positive staining in each group. TRAP⁺ cells were mainly located on the defect edge in the Control and LPS groups, while they were mainly located around the biomaterials in the IL4 group (red arrow). E) IHC staining of MNGCs. CD206⁺ MNGCs could be observed in the IL4 group, while CCR7⁺ MNGCs could be observed in the LPS group (green arrow). M: materials; PDL: periodontal ligament; AB: alveolar bone (* control vs. LPS/IL4 group, # LPS vs. IL4 group, $p < 0.05$).

changed to an anti-inflammatory status. The connecting lines between upregulated immune factors and the regenerative factors in LPS group became dense, implying closer connection of the upregulation immune factors and the regenerative factors. The expression level of multiple regenerative factors also increased, accounting for the observed tissue regeneration (Fig. 5D). MMP9 and MMP13 can degrade extracellular matrix and collagen fibers [44]. The up-regulation of MMP9 and MMP13, implying the absorption of necrotic tissues and tissue remodeling. COL1A1 and IGF1 are related to fiber formation process [45–47]. The increase of COL1A1 and IGF1 suggesting the improved fiber synthesis activity. As an angiogenic factor, PDGF was upregulated, which implied an active angiogenesis [48]. Moreover, the osteogenic potency was also improved with the increase in the osteogenic and related factors,

including BMP2, OPG, OPN, MGP, and SPOCK1, in this period [49–51].

In the IL4 group, the expression levels of multi-tissue regenerative factors were also closely related with the local anti-inflammatory immune environment on day 3 (Fig. 5A). The fiber remodeling-related factors COL1A1 and MMP13 and the angiogenic factor PDGF were highly expressed in the IL4 group [48] (Fig. 5C). POSTN, OPN, IGF1, OPG, COL1A1, and SPOCK1 have been known as osteogenic related factors [47,51]. The increased expression of them suggested the promotion of osteoblast migration, differentiation, and bone matrix mineralization. Furthermore, MGP, SPOCK1, and OPN known as cementum mineralization-related cellular factors [51], the upregulation of them indicated an increase in cementoblast differentiation and cementum mineralization. IGF1, COL1A1, PDGF, and FGFR2 have been found to

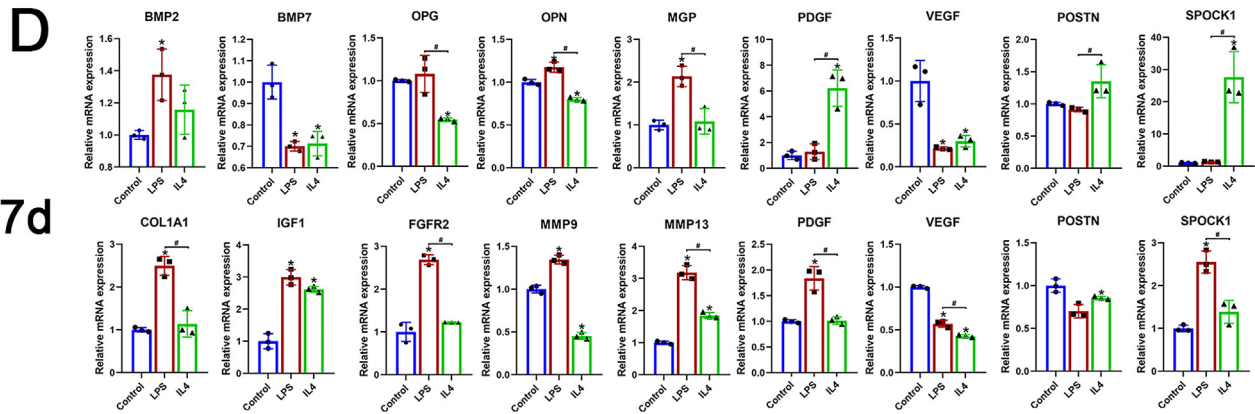
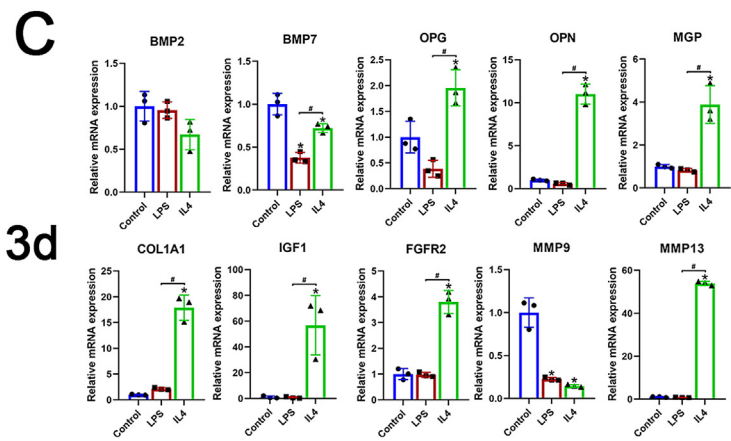
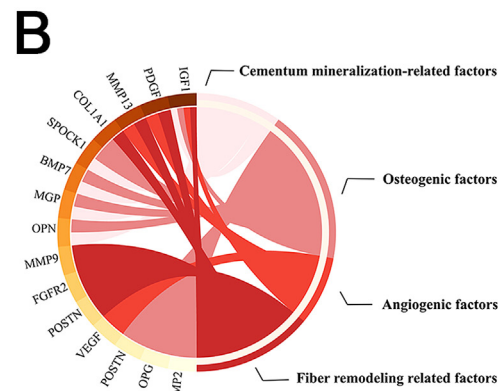
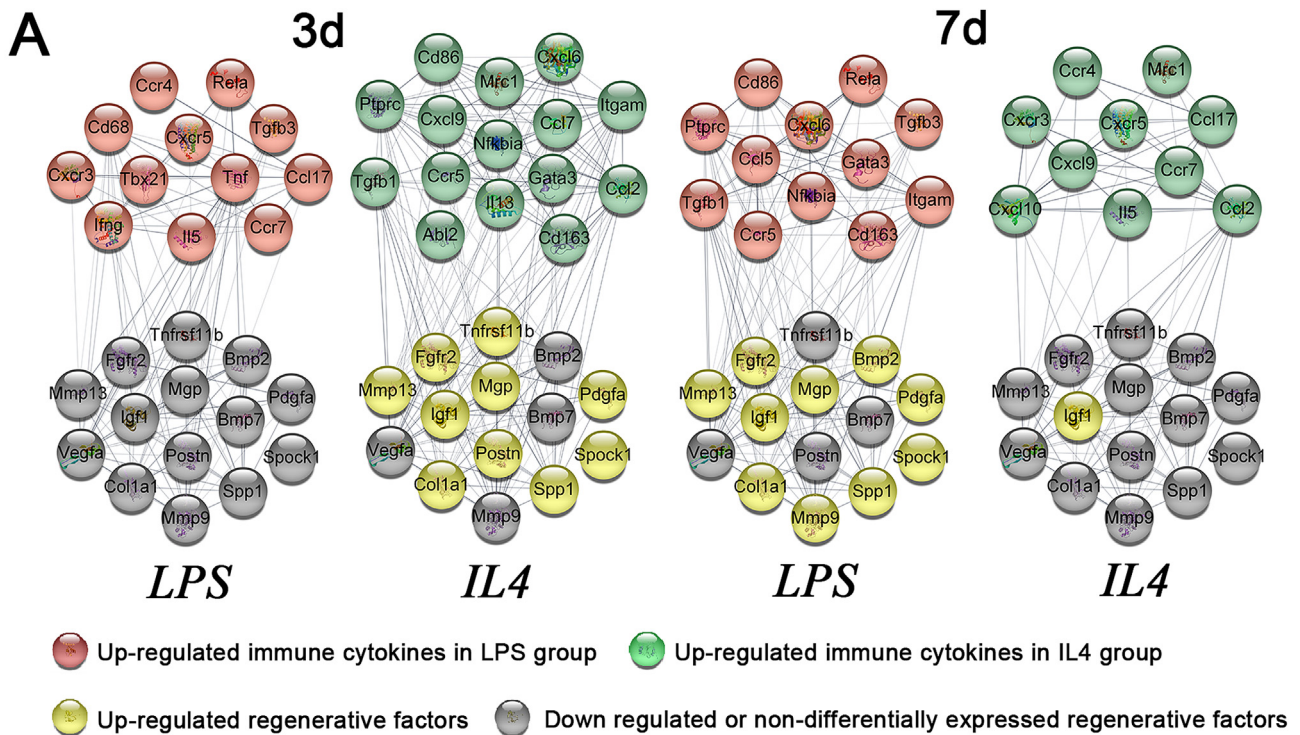


Fig. 5. The effects of the generated immune microenvironments on the multi-tissue regeneration regulatory factors. A) Protein interaction analysis of the up-regulated immune cytokines and typical multi-tissue regeneration-related factors in each group, showing a close regulatory effect. The red spheres represent the up-regulated immune cytokines in LPS group, the green spheres represent the up-regulated immune cytokines in IL4 group, the yellow spheres represent the up-regulated regenerative factors in gene expression relative to the Control group. The gray spheres are down-regulated or non-differentially expressed regenerative factors in gene expression relative to the control group. B) Function annotation of the multi-tissue regeneration-related factors. C-D) Gene expression level of the multi-tissue regeneration-related factors at day 3 and 7. (* control vs. LPS/IL4 group, # LPS vs. IL4 group, $p < 0.05$).

participate in fibroblast migration and differentiation, while MMP13 is involved in collagen degradation [52,53]. The significant increase in the IGF1, COL1A1, PDGF, FGFR2, and MMP13 levels indicated an active remodeling of the ECM and the collagen fibers in the IL4 group.

As the multi-tissue regeneration progressed, the growth factor levels did not show a significant increase at day 7 (Fig. 5D). According to results 2.2.1, the IF staining results shows the amount of CD90⁺ CD34⁻ cells in the IL4 group was obviously higher than that in the other groups (Fig. 2D), all these results suggest a superior outcome of multi-tissue regeneration in the further regenerative stage.

In summary, the immunopathophysiological process induced by biomaterials is closely related to the immunoregulatory performance of the implanted biomaterials. The implantation of cell-free biomaterials with proinflammatory properties could initially generate a type 1 proinflammatory microenvironment locally by causing excessive blood clot fibrin accumulation and fibrinoid necrosis, releasing proinflammatory factors, inducing the involvement of M1 macrophages and MNGCs, activating Th1 and recruiting B cells. The adaptive immune response included the activation of Th1 and the recruitment of B cells. The participants of the adaptive immune reaction implied the involvement of the systemic immune systems. This microenvironment resulted in multi-tissue regeneration-related factors, which regulated the subsequent multi-tissue regeneration. However, when the microenvironment shifted towards a type 2 wound healing immune microenvironment, the levels multi-tissue regenerative factors increased, indicating the beginning of the regeneration process. Moreover, the cell-free biomaterials with anti-inflammatory properties could initially generate a type 2 wound healing microenvironment and start the multi-tissue regeneration process.

2.3. The involvement of systemic immune response in this immunopathophysiological process

Systemic immune response could play an important role in local tissue regeneration. Activated antigen-presenting cells, cytokines, chemical irritant in local area could induce immune responses in peripheral immune organs including lymph nodes and spleen through lymphatic fluid and blood circulation respectively [54,55]. Systemic derived cells could further modulate the local environment via releasing cytokines and migrating to local area. As mentioned in section 2.2, the upregulation of T cell chemotactic factors and T cell markers could be detected, suggesting the involvement of the immune system. Thus, the investigation of the involvement of systemic immune response in the generation of local immune microenvironment is becoming attractive. The systemic toxicity of the implanted biomaterials was first tested to exclude the biosafety and the so-caused toxicity effect. A non-toxic reaction was observed in all the tested organs for all the observation times (Supplementary Fig. 2).

No obvious anatomic and histological difference was observed in each group in lymph node at day 3 (Fig. 6A). As for the LPS group, proinflammatory cytokines such as TNF α , IL1, IL6 were both up-regulated (Fig. 6B). Enriched terms included inflammatory response and LPS response (Fig. 6C). These all suggested a pro-inflammatory status, which was similar with the local area response. As the receptor of LPS, TLR4 was up-regulated, leading to the activation of NF κ B and consequent transcription of pro-inflammatory cytokines including TNF α , IL1, and IL6, which can promote T cell maturation and Th1 differentiation [56]. Th1 marker Tbx21 was also up-regulated. With the upregulation of chemokines, such as CXCR5, CXCR3, and CCR5, the cell migration and interaction activity in the lymph nodes was enhanced and T cell maturation could be further improved. At day 7, the LPS-related proinflammatory response was decreased and a homeostasis status was reached once again (Fig. 6D–F). The immune response of the spleen was not as intense as that in the lymph nodes, with no obvious anatomic and histological change at day 3 and 7 (Fig. 6G, J). TLR4 and the related proinflammatory cytokines

were only slightly upregulated at day 3 and became more weakened at day 7 with the upregulation of only a few anti-inflammatory cytokines (Fig. 6H, K). Interestingly, the GO analysis results all suggest the positive regulation of an isotype switch to the IgG isotype was activated at day 3 and 7 (Fig. 6I, L), which suggest the increasement of IgG. As an important component of humoral immunity, IgG could activate complements and neutralize toxins, thus promoting antigen-antibody reaction [57].

A different systemic immune response was observed in the IL4 group. In lymph nodes, the immune status tends to be more anti-inflammatory with the upregulation of the anti-inflammatory cytokines CD163, Arg, IL5, TGF β 1 and TGF β 3 at day 3 (Fig. 6B). IL5 can be synthesized and secreted mainly by activated CD4⁺ helper T cells of the T-helper-2 (Th2) [58]. TGF β family could regulate the activation and phenotypes transformation [59]. The up-regulation of IL5, TGF β 1, and TGF β 3 suggest the promotion of T cell activation and differentiation. The GO enriched term also included T cell differentiation and T cell receptor signaling pathway (Fig. 6C). At day 7, chemokines including CXCL6 and CXCL10 were both up-regulated (Fig. 6E), suggesting active cell migration activity. The GO analysis suggested the positive regulation of JAK-STAT cascade (Fig. 6F), which could be activated by IL2 and IL5, and further regulating the immune response [60]. The enhanced migration ability was corresponded with the upregulation of T cell chemokines in local area, as mentioned above. Interestingly, unlike the anti-inflammatory immune environment in the lymph nodes, the immune response in the spleen tends to be related with the inflammatory response and LPS response, which lasted from day 3–7, as suggested by the gene expression heatmap and gene ontology (GO) analysis results (Fig. 6G–L). Degradation of necrotic tissue activity in local area might have been the stimulation source of pro-inflammatory response of spleen in the IL4 group.

From our results, the immune response in the adjacent lymph nodes seemed to be enlarged and to supplement the local immune response and participated in the generation of the local immune microenvironment. After activating the local immune response, the antigens could be presented through the lymph and cause the corresponding T cell and B cell response in the lymph nodes [61]. The activated T cells and B cells could be recruited by the chemokines to the local site and were involved in the generation of the local immune microenvironment [18]. However, the immune response in the spleen can be activated by blood-borne stimulation; thus, the signals from the local area may cascade through blood circulation and be influenced by multiple factors, which complicates the interaction between the spleen and the local defect area [62,63].

2.4. The periodontal multi-tissue regeneration outcomes

Four weeks after the surgery, the periodontal multi-tissue regeneration effect was analyzed. An overview of the periodontal regeneration outcome was obtained via micro-CT and H&E staining. In the LPS group, the overall multi-tissue regeneration effect was inferior (Fig. 7A and B). The Goldner staining results show sparse collagenous formations and no obvious ALP positive cells were observed in the LPS group, indicating a worse bone formation effect than in the other two groups (Fig. 7C and D). The perforating fiber, named as Sharpey's fiber, is a unique structure in periodontal tissue, and its formation is highly oriented and can be observed via PR staining combined with polarized light microscopy [64, 65]. However, the formation of Sharpey's fibers was hardly observed in the LPS group (Fig. 7E). OPN and BSP are the main noncollagenous proteins of cementum [51]. The sign of cementum regeneration in the LPS group was inconspicuous, since no obvious OPN and BSP positive staining was observed (Fig. 7E–G).

However, a better multi-tissue regeneration was observed in the IL4 group. Superior bone formation in the IL4 group was found in the micro-CT, H&E staining, and Goldner's staining results (Fig. 7A–C). Moreover, ALP positive cells were found on the edge of new bone and in the dentin defect surface (Fig. 7D), suggesting an active osteogenesis activity and

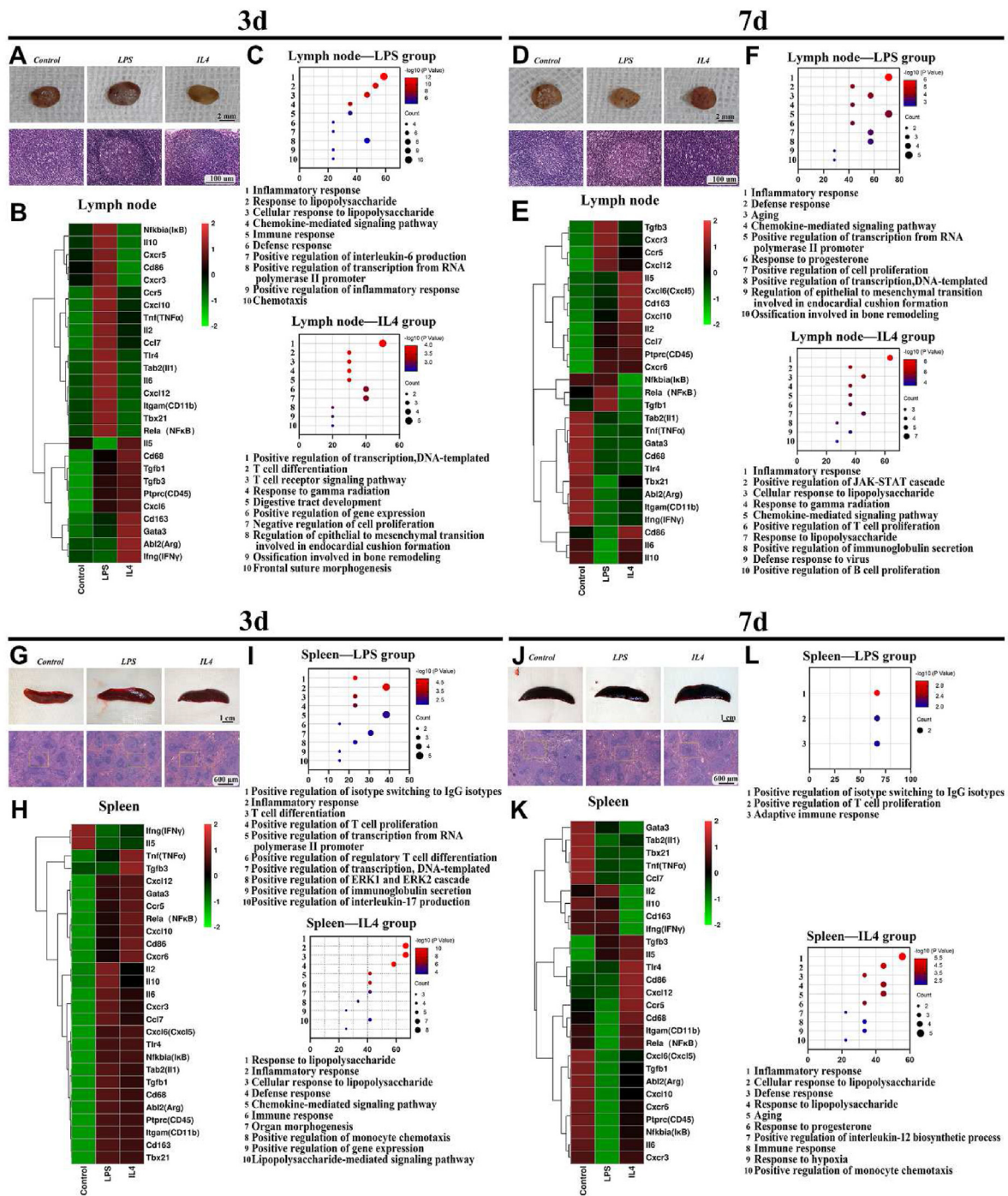


Fig. 6. Systemic immune response involved in the tissue regeneration process at day 3 and 7. A, D) Histological analysis of the lymph nodes at day 3 and 7. B, E) Gene expression heatmap of the immune factors of the lymph nodes at day 3 and 7. C, F) GO-BP analysis of the highly expressed genes in the lymph nodes at day 3 and 7. G, J) Histological analysis of the spleen at day 3 and 7. H, K) Gene expression heatmap of the immune factors in the spleen at day 3 and 7. I, L) GO-BP analysis of the highly expressed genes in the spleen at day 3 and 7.

the potential formation of perforating fibers and acellular cementum in the IL4 group. The PR staining results show the highly organized and parallel newly formed periodontal fibers extending from newly formed alveolar bone to the root surface (Fig. 7E). OPN positive staining was also observed in newly formed woven bone, periodontal fibers, and in the root surface in the IL4 group (Fig. 7F). Continuous BSP positive bands were also observed on the surface of dentin and were closely attached to the root surface in the IL4 group (Fig. 7G). Herein, the regeneration of alveolar bone, Sharpey's fibers, and cementum-like structures was observed in the IL4 group.

2.5. Implications for the development of advanced immunomodulatory multi-tissue regenerative materials

In summary, cell-free biomaterials with pro- or anti-inflammatory properties effectively regulate the acute injury reaction. The effects of the immune microenvironment on the periodontal tissue were initially elicited by regulating the fibrin network and the formation of fibrinoid necrosis in the periodontal ligament tissue. Polarization macrophages, MNGCs, and the adaptive immune response, which is regulated by the systemic immune reaction, were subsequently involved in generating and

In situ multi-tissue regeneration mediated by cell-free immunomodulatory biomaterials and their immunopathophysiological processes

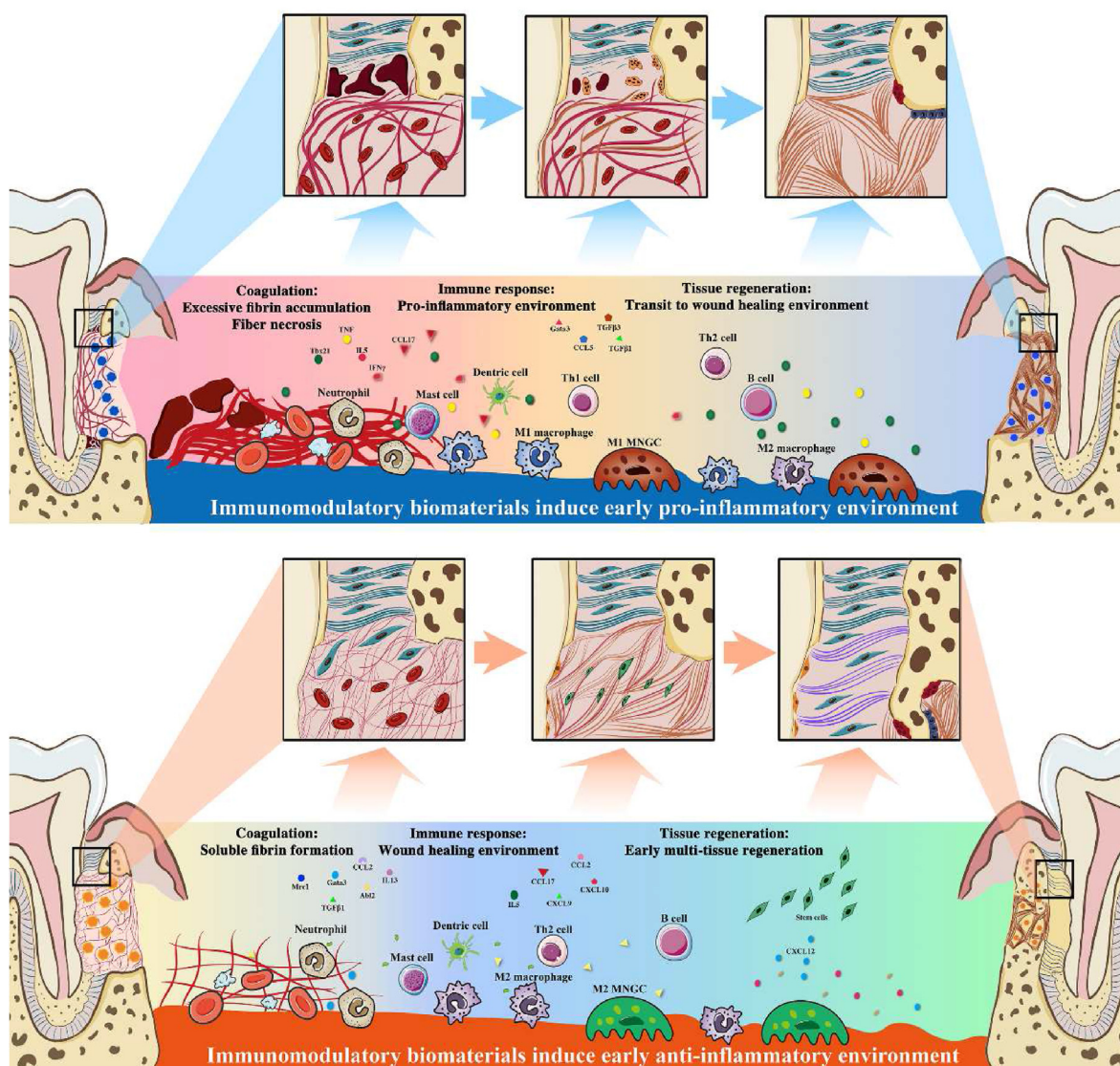


Fig. 8. Schematic figure: the immunopathophysiological processes for periodontal multi-tissue regeneration triggered by different cell-free immunomodulatory biomaterials were characterized by a complex set of biological events of the acute injury histological reaction, the phenotype transition of innate immune cell subsets, the involvement of the systemic immune reaction, the interaction of immune cytokines, the expression of growth factors and the recruitment of stem cells, from the acute injury reactive phase to the tissue remodeling stage.

regenerative capacity among different groups was observed in the early stage, and early immune regulation would be effective for multi-tissue regeneration.

However, our study preliminary demonstrated the discrepant immunopathophysiological process of pro-inflammatory and anti-inflammatory immunomodulatory biomaterials *in vivo*. Further researches need to be done to reveal the dose effect or the combination effect of immunomodulatory effectors and their underlying mechanisms. Secondly, the evaluation of periodontal complex regeneration was complex and difficult. Especially in observing the new-formed cementum, because of the limitation detection method. Therefore, an evaluation system for periodontal multi-tissue regeneration *in vivo* was needed to be established. Approaches applied in this study could generally satisfy the needs of comparing the effect of periodontal regeneration. However, more specific, powerful and straightforward evaluation method should be developed. Finally, the immune cytokines and growth

factors analyzed in this study may not completely and accurately depict the full view of the immunopathophysiological process. With further research in the future, more specific and comprehensive conclusion could be made. The specific immunopathophysiological process may vary according to different materials, but the immune reaction of materials with similar immunomodulatory function may follow similar pattern.

3. Conclusion

Our results showed that the outcome of multi-tissue regeneration is closely regulated by the immune reaction. The underlying immunopathophysiological process, including the involvement of a blood clotting response and fibrinoid necrosis, innate and adaptive immune response, local and systemic immune reaction, growth factor release, and stem cell recruitment, was revealed. From our results, the implantation of biomaterials with anti-inflammatory properties could direct the

immunopathophysiological process towards one that is more favorable for *in situ* multi-tissue regeneration, and ultimately lead to the regeneration of periodontal ligament, acellular cementum matrix, and alveolar bone in the periodontium. This constitutes a promising strategy to developed cell-free biomaterials for *in situ* multi-tissue regeneration.

4. Experimental section

4.1. Preparation of the PHA and PDA-PHA

Porcine hydroxyapatite (PHA) was prepared according to our previous studies [68,69]. Briefly, cancellous bone harvested from the porcine femoral epiphysis was immersed in 30% H₂O₂ and 75% ethanol respectively for 24 h to remove soft tissues. The bones were dissected into regular blocks (10 mm*10 mm*5 mm dimensions) by cut-off machines (Accutom-50, Struers, Ballerup, Denmark) and calcined at 800 °C for 2 h in a muffle furnace (SGM6812BK, Sigma Furnace Industry, China). The PHA blocks were then grinded into particles and filtered by screen with 0.2 mm and 0.5 mm hole size to obtain 0.2–0.5 mm PHA particles. Image J has been performed to measure the maximum and minimum Feret diameter of the PHA particles. For PDA coating formation, dopamine hydrochloride (Sigma, USA) was dissolved in a 0.01 M Tris-base solution (Sigma, USA) to obtain a 2 mg/mL polydopamine (PDA) solution. The PHA particles were immersed in the PDA solution for 48 h to form a PDA nano coating on PHA (PDA-PHA). Next, SEM, FTIR, XRD, and XPS were used to characterize the biomaterials.

4.2. Immobilization of immune modulatory factors

The PDA-PHAs were dipped in an LPS (10 µg/mL, InvivoGen, FRA) + IFN γ (200 ng/mL, R&D Systems, USA) or an IL4 (500 ng/mL, R&D Systems, USA) solution for 24 h at 4 °C to obtain LPS/IFN γ -PDA-PHA (LPS group) and IL4-PDA-PHA (IL4 group). ELISA and LPS endotoxin assays were performed to detect the concentration of IL4, LPS, and IFN γ remaining in the stimulation solution to verify the loading amounts. Immunofluorescence staining was performed to visualize the distribution of LPS/IFN γ and IL4 on the PDA-PHA particles. Firstly, PDA-PHA was incubated with FITC-LPS+IFN γ and IL4 solution as above mentioned. After medium removed, materials were incubated with Alexa Fluor® 647 anti-rat IFN γ Antibody, eFluor 660 IL4-Monoclonal Antibody at 4 °C for 2 h. The samples were observed under a fluorescence microscope.

4.3. Animal surgery

Male Sprague–Dawley rats aged six to eight weeks were used to observe the tissue regeneration process and evaluate the multi-tissue regeneration effect. The animal surgical protocols followed were approved by the Institutional Animal Care and Use Committee of Sun Yat-sen University. The periodontal defect model was prepared according to a previously published protocol, with some modifications [27]. Briefly, rats were anesthetized and 1 cm skin incision was made along the oral horn to ear. Masseter was exposed and two distinct anatomical landmarks (parotid duct and facial nerve) could be seen on the surface of masseter. The masseter was cut parallel to the parotid duct and facial nerve to reach the buccal bone. A periodontal defect (5 × 2 × 1 mm) was prepared with a 1.8 mm diameter drill. The size of defect was measured by a periodontal probe. After anesthesia, a periodontal defect was prepared on the buccal alveolar bone on the posterior tooth area of the rat mandible. The prepared PDA-PHA (control group), LPS/IFN γ -PDA-PHA (LPS group), and IL4-PDA-PHA (IL4 group) were implanted into the defect area (n = 6). The animals were sacrificed at 3 days, 7 days, and 4 weeks for further analysis.

4.4. Acute injury reaction and the initial multi-tissue repair process

At day 3 and 7, the mandibles were collected to analyze their

histology. After fixation, the mandibles were decalcified in a 10% EDTA solution (pH 7.4) for four weeks. For H&E staining, the nuclei were stained with Mayer's hematoxylin (Servicebio, China), and the cytoplasm was stained with eosin (Servicebio, China). For Martius scarlet blue (MSB) staining, the red blood cells were stained with the Martius solution, the fibrin was stained with the Ponceau staining solution, and the collagen was stained with aniline blue (Pythonbio, China). Quantification analysis of blood clot fibrin thickness at day 3 was conducted by Image J software. For IHC staining, the slides were blocked with a 5% BSA (Macklin, China) solution for 1 h and incubated with ALP (1:100, Abcam, UK) after antigen retrieval. The sections were then incubated with a secondary antibody (Genetech, China) for 30 min at room temperature. The diaminobenzidine solution (Genetech, China) and Mayer's hematoxylin were used to stain the antigen-antibody complexes and the nuclei. For immunofluorescence staining, after antigen retrieval, the slides were blocked with a 5% BSA solution for 1 h and incubated with mouse anti-CD68 (1:100, Invitrogen, USA), rabbit anti-CCR7 (1:100, Abcam) and rabbit anti-D206 (1:10,000, UK) at 4 °C overnight. Donkey anti-rabbit IgG (1:100, Beyotime, China) or goat anti-mouse IgG (1:100, EMAR, China) was used as a secondary antibody and the nuclei were stained using 2-(4-amidinophenyl)-6-indolecarbamide dihydrochloride (DAPI, Beyotime, China). Immunofluorescence staining of rabbit anti-CD34 (1:100, Abcam, UK) and mouse anti-CD90 (1:100, Abcam, UK) was conducted as mentioned above for identifying the stem cells in the local area. Images were captured using Aperio AT2 system and a fluorescence microscope.

4.5. Characterization of the immune microenvironment

At day 3 and 7, blood clots at the defect area were collected for RNA extraction. The gene expression of immune cytokines was assessed using RT-qPCR, as previously described [16]. The RT-qPCR primers used in this study are listed in Supplementary Table 1. Advanced heatmap plotting was performed using the OmicStudio tools at <https://www.omicstudio.cn>. The cytokines interaction network was further obtained using Cytoscape software (3.7.2) based on the String database. IHC staining of CD68 (1:100, Abcam, UK), CCR7 (1:100, Abcam, UK), and CD206 (1:10,000, Abcam, UK) was conducted as mentioned above. TRAP staining was performed to analyze the MNGCs, as previously described [16]. After being washed with pure water, the slices were counterstained with Mayer's hematoxylin. Images were captured using an Aperio AT2 system and semi-quantification was conducted using Image J software (1.46).

4.6. Multi-tissue repair process initiated by different immunomodulatory biomaterials

The expression levels of multi-tissue-related genes were detected and quantified using RT-qPCR. Cytoscape software was used to analyze the interaction between the highly expressed factors in the LPS and IL4 groups and the downstream multi-tissue regenerative factors (based on the String database).

4.7. Evaluation of the systemic immune response

For systemic toxicity analysis, the liver, kidneys, brain, and heart were collected for systemic toxicity evaluation at each time point. The sectioning and H&E staining of samples was conducted as mentioned above. Images were captured and analyzed using an Aperio AT2 system. For immune environment analysis, the spleen and superficial cervical lymph nodes were collected for RNA extraction. The gene expression of immune cytokines was assessed using RT-qPCR. The gene expression heatmaps were prepared and analyzed via online software program Omicstudio (<https://www.omicstudio.cn/index>).

4.8. Evaluation of the periodontal multi-tissue regeneration

At 4 weeks, the mandible was collected to analyze the multi-tissue regeneration effect. After fixing it with 4% paraformaldehyde for 24 h, the tissue was scanned using a micro-CT scanner (μ CT50; SCANCO Medical AG, Switzerland). Materialize Mimics Research 19 (Materialize, Belgium) software was used to reconstruct the three-dimensional images. The mandible was further decalcified in a 10% EDTA solution (pH 7.4) for four weeks and H&E staining was performed. For Goldner's trichrome staining, the slices were first stained with hematoxylin for 20 min, followed by staining with fuchsin acid, orange G, fuchsin acid, and light green stain for 5–10, 1–5, 3–5, and 3–10 min, respectively (Servicebio, China). For picrosirius red staining, the paraffin sections were impregnated with picrosirius red (Servicebio, China) for 10 min and differentiation was induced with ethanol for 3 s. IHC staining of ALP (1:100, Abcam, UK), OPN (1:200, Abcam, UK), and BSP (1:200, Abcam, UK) was performed as previously described. The sections were scanned using an Aperio AT2 system. The picrosirius red-stained sections were observed and photographed using a polarized light microscope.

4.9. Statistical analysis

The experimental results are presented as mean \pm standard deviation. GraphPad Prism 8 was used for statistical analysis. One-way ANOVA with Tukey's HSD analysis was used to compare the differences between the groups. The statistical significance was set as $p < 0.05$.

Credit author statement

Guanqi Liu: Conceptualization, Methodology, Formal analysis, Investigation, Writing - Original Draft, Writing - Review & Editing, Visualization, Supervision, Funding acquisition, **Xuan Zhou:** Methodology, Formal analysis, Investigation, Writing - Original Draft, Visualization, **Linjun Zhang:** Methodology, Formal analysis, Investigation, Writing - Original Draft, Visualization, **Yang Zou:** Methodology, Formal analysis, **Junlong Xue:** Methodology, Formal analysis, Visualization, **Ruidi Xia:** Formal analysis, Visualization, **Nuerbiya Abuduxiku:** Visualization, **Xuejing Gan:** Visualization, **Runheng Liu:** Methodology, **Zhuofan Chen:** Conceptualization, Project administration, **Yang Cao:** Conceptualization, Project administration, **Zetao Chen:** Conceptualization, Writing - Review & Editing, Supervision, Project administration, Funding acquisition.

Declaration of competing interest

The authors declare that they have no known competing financial interests or personal relationships that could have appeared to influence the work reported in this paper.

Data availability

All data needed to evaluate the conclusion in the paper are present in the paper and/or the supplementary Materials. Additional data related to this paper may be requested from authors.

Acknowledgements

This work was financially funded by the National Natural Science Foundation of China (82071167), Natural Science Foundation of Guangdong Province (2018B030306030), China Postdoctoral Science Foundation (2020M680139), Guangdong Basic and Applied Basic Research Foundation (2020A1515110180), Guangdong Financial Fund of High-Caliber Hospital Construction.

Appendix A. Supplementary data

Supplementary data to this article can be found online at <https://doi.org/10.1016/j.mtbio.2022.100432>.

References

- [1] A. Nanci, D.D. Bosshardt, Structure of periodontal tissues in health and disease, *Periodontol.* 40 (2006) 11–28, 2000.
- [2] N. Yan, B. Hu, J.C. Xu, R. Cai, Z.H. Liu, D.P. Fu, et al., Stem cell Janus patch for periodontal regeneration, *Nano Today* 42 (2022).
- [3] S.H. Bassir, W. Wisitrasameewong, J. Raanan, S. Ghaffarigarakani, J. Chung, M. Freire, et al., Potential for stem cell-based periodontal therapy, *J. Cell. Physiol.* 231 (2016) 50–61.
- [4] F.M. Chen, J. Zhang, M. Zhang, Y. An, F. Chen, Z.F. Wu, A review on endogenous regenerative technology in periodontal regenerative medicine, *Biomaterials* 31 (2010) 7892–7927.
- [5] C.H. Evans, G.D. Palmer, A. Pascher, R. Porter, F.N. Kwong, E. Gouze, et al., Facilitated endogenous repair: making tissue engineering simple, practical, and economical, *Tissue Eng.* 13 (2007) 1987–1993.
- [6] Z. Yang, H. Li, Z. Yuan, L. Fu, S. Jiang, C. Gao, et al., Endogenous cell recruitment strategy for articular cartilage regeneration, *Acta Biomater.* 114 (2020) 31–52.
- [7] Y. Wang, X. Chen, W. Cao, Y. Shi, Plasticity of mesenchymal stem cells in immunomodulation: pathological and therapeutic implications, *Nat. Immunol.* 15 (2014) 1009–1016.
- [8] L.L. Chen, G.Q. Liu, J.Y. Wu, X. Zhou, Y.M. Zhao, Z.T. Chen, et al., Multi-faceted effects of mesenchymal stem cells (MSCs) determined by immune microenvironment and their implications on MSC/biomaterial-based inflammatory disease therapy, *Appl. Mater. Today* 18 (2020).
- [9] Z.T. Chen, T. Klein, R.Z. Murray, R. Crawford, J. Chang, C.T. Wu, et al., Osteoimmunomodulation for the development of advanced bone biomaterials, *Mater. Today* 19 (2016) 304–321.
- [10] M. Rodrigues, N. Kosaric, C.A. Bonham, G.C. Gurtner, Wound healing: a cellular perspective, *Physiol. Rev.* 99 (2019) 665–706.
- [11] A.K. Gaharwar, I. Singh, A. Khademhosseini, Engineered biomaterials for in situ tissue regeneration, *Nat. Rev. Mater.* 5 (2020) 686–705.
- [12] Z. Chen, S. Ni, S. Han, R. Crawford, S. Lu, F. Wei, et al., Nanoporous microstructures mediate osteogenesis by modulating the osteo-immune response of macrophages, *Nanoscale* 9 (2017) 706–718.
- [13] C. Wu, Z. Chen, D. Yi, J. Chang, Y. Xiao, Multidirectional effects of Sr-, Mg-, and Si-containing bioceramic coatings with high bonding strength on inflammation, osteoclastogenesis, and osteogenesis, *ACS Appl. Mater. Interfaces* 6 (2014) 4264–4276.
- [14] E. Boanini, P. Torricelli, M. Fini, A. Bigi, Osteopenic bone cell response to strontium-substituted hydroxyapatite, *J. Mater. Sci. Mater. Med.* 22 (2011) 2079–2088.
- [15] Z. Chen, J. Yuen, R. Crawford, J. Chang, C. Wu, Y. Xiao, The effect of osteoimmunomodulation on the osteogenic effects of cobalt incorporated beta-tricalcium phosphate, *Biomaterials* 61 (2015) 126–138.
- [16] G.Q. Liu, X.S. Wang, X. Zhou, L.J. Zhang, J.M. Mi, Z.J. Shan, et al., Modulating the cobalt dose range to manipulate multisystem cooperation in bone environment: a strategy to resolve the controversies about cobalt use for orthopedic applications, *Theranostics* 10 (2020) 1074–1089.
- [17] D.N. Morand, J.L. Davideau, F. Clauss, N. Jessel, H. Tenenbaum, O. Huck, Cytokines during periodontal wound healing: potential application for new therapeutic approach, *Oral Dis.* 23 (2017) 300–311.
- [18] Z. Julier, A.J. Park, P.S. Briquez, M.M. Martino, Promoting tissue regeneration by modulating the immune system, *Acta Biomater.* 53 (2017) 13–28.
- [19] M. Camelo, M.L. Nevins, S.E. Lynch, R.K. Schenk, M. Simion, M. Nevins, Periodontal regeneration with an autogenous bone-Bio-Oss composite graft and a Bio-Gide membrane, *Int. J. Periodontics Restor. Dent.* 21 (2001) 109–119.
- [20] D.D. Bosshardt, A. Sculean, Does periodontal tissue regeneration really work? *Periodontology* 51 (2009) 208–219, 2000.
- [21] R. Liu, W. Qiao, B. Huang, Z. Chen, J. Fang, Z. Li, et al., Fluorination enhances the osteogenic capacity of porcine hydroxyapatite, *Tissue Eng.* 24 (2018) 1207–1217.
- [22] Y.B. Lee, Y.M. Shin, J.H. Lee, I. Jun, J.K. Kang, J.C. Park, et al., Polydopamine-mediated immobilization of multiple bioactive molecules for the development of functional vascular graft materials, *Biomaterials* 33 (2012) 8343–8352.
- [23] H. Lee, J. Rho, P.B. Messersmith, Facile conjugation of biomolecules onto surfaces via mussel adhesive protein inspired coatings, *Adv. Mater.* 21 (2009) 431–434.
- [24] F. Lebre, R. Sridharan, M.J. Sawkins, D.J. Kelly, F.J. O'Brien, E.C. Lavelle, The shape and size of hydroxyapatite particles dictate inflammatory responses following implantation, *Sci. Rep.* 7 (2017) 2922.
- [25] L.M. Atayde, P.P. Cortez, A. Afonso, M. Santos, A.C. Mauricio, J.D. Santos, Morphology effect of bioglass-reinforced hydroxyapatite (Bonelike(R)) on osteoregeneration, *J. Biomed. Mater. Res. B Appl. Biomater.* 103 (2015) 292–304.
- [26] M. Padiál-Molina, J.T. Marchesan, A.D. Taut, Q. Jin, W.V. Giannobile, H.F. Rios, Methods to validate tooth-supporting regenerative therapies, *Methods Mol. Biol.* 887 (2012) 135–148.
- [27] M. Padiál-Molina, J.C. Rodriguez, S.L. Volk, H.F. Rios, Standardized in vivo model for studying novel regenerative approaches for multitissue bone-ligament interfaces, *Nat. Protoc.* 10 (2015) 1038–1049.

- [28] H.T. Shiu, B. Goss, C. Lutton, R. Crawford, Y. Xiao, Formation of blood clot on biomaterial implants influences bone healing, *Tissue Eng Part B Rev* 20 (2014) 697–712.
- [29] B.N. Brown, B.D. Ratner, S.B. Goodman, S. Amar, S.F. Badylak, Macrophage polarization: an opportunity for improved outcomes in biomaterials and regenerative medicine, *Biomaterials* 33 (2012) 3792–3802.
- [30] K. Sadtler, K. Estrellas, B.W. Allen, M.T. Wolf, H. Fan, A.J. Tam, et al., Developing a pro-regenerative biomaterial scaffold microenvironment requires T helper 2 cells, *Science* 352 (2016) 366–370.
- [31] A. Mantovani, S.K. Biswas, M.R. Galdiero, A. Sica, M. Locati, Macrophage plasticity and polarization in tissue repair and remodelling, *J. Pathol.* 229 (2013) 176–185.
- [32] J.P. Luyendyk, J.G. Schoenecker, M.J. Flick, The multifaceted role of fibrinogen in tissue injury and inflammation, *Blood* 133 (2019) 511–520.
- [33] R.J. Miron, D.D. Bosshardt, Multinucleated giant cells: good guys or bad guys? *Tissue Eng. Part B Rev.* 24 (2018) 53–65.
- [34] T.T. Lau, D.A. Wang, Stromal cell-derived factor-1 (SDF-1): homing factor for engineered regenerative medicine, *Expert Opin. Biol. Ther.* 11 (2011) 189–197.
- [35] X. Huang, B. Guo, S. Liu, J. Wan, H.E. Broxmeyer, Neutralizing negative epigenetic regulation by HDAC5 enhances human haematopoietic stem cell homing and engraftment, *Nat. Commun.* 9 (2018) 2741.
- [36] Q. Liang, L. Du, R. Zhang, W. Kang, S. Ge, Stromal cell-derived factor-1/Exendin-4 cotherapy facilitates the proliferation, migration and osteogenic differentiation of human periodontal ligament stem cells in vitro and promotes periodontal bone regeneration in vivo, *Cell Prolif* 54 (2021), e12997.
- [37] A. Schindeler, M.M. McDonald, P. Bokko, D.G. Little, Bone remodeling during fracture repair: the cellular picture, *Semin. Cell Dev. Biol.* 19 (2008) 459–466.
- [38] F. Loi, L.A. Cordova, J. Pajarinen, T.H. Lin, Z. Yao, S.B. Goodman, Inflammation, fracture and bone repair, *Bone* 86 (2016) 119–130.
- [39] M.C. Groeneveld, V. Everts, W. Beertsen, A quantitative enzyme histochemical analysis of the distribution of alkaline phosphatase activity in the periodontal ligament of the rat incisor, *J. Dent. Res.* 72 (1993) 1344–1350.
- [40] M.C. Groeneveld, V. Everts, W. Beertsen, Alkaline phosphatase activity in the periodontal ligament and gingiva of the rat molar: its relation to cementum formation, *J. Dent. Res.* 74 (1995) 1374–1381.
- [41] M.C. Groeneveld, V. Everts, W. Beertsen, Formation of afibrillar acellular cementum-like layers induced by alkaline phosphatase activity from periodontal ligament explants maintained in vitro, *J. Dent. Res.* 73 (1994) 1588–1592.
- [42] M.G. Kazanietz, M. Durando, M. Cooke, CXCL13 and its receptor CXCR5 in cancer: inflammation, immune response, and beyond, *Front. Endocrinol.* 10 (2019) 471.
- [43] B.N. Brown, J.E. Valentin, A.M. Stewart-Akers, G.P. McCabe, S.F. Badylak, Macrophage phenotype and remodeling outcomes in response to biologic scaffolds with and without a cellular component, *Biomaterials* 30 (2009) 1482–1491.
- [44] K.B.S. Paiva, J.M. Granjeiro, Matrix metalloproteinases in bone resorption, remodeling, and repair, *Prog Mol Biol Transl Sci* 148 (2017) 203–303.
- [45] S. Lin, Q. Zhang, X. Shao, T. Zhang, C. Xue, S. Shi, et al., IGF-1 promotes angiogenesis in endothelial cells/adipose-derived stem cells co-culture system with activation of PI3K/Akt signal pathway, *Cell Prolif* 50 (2017).
- [46] P. Shah, L. Keppler, J. Rutkowski, A review of platelet derived growth factor playing pivotal role in bone regeneration, *J. Oral Implantol.* 40 (2014) 330–340.
- [47] R. Marsell, T.A. Einhorn, The biology of fracture healing, *Injury* 42 (2011) 551–555.
- [48] P.C. Smith, C. Martinez, J. Martinez, C.A. McCulloch, Role of fibroblast populations in periodontal wound healing and tissue remodeling, *Front. Physiol.* 10 (2019) 270.
- [49] I. Grafe, S. Alexander, J.R. Peterson, T.N. Snider, B. Levi, B. Lee, et al., TGF-Beta family signaling in mesenchymal differentiation, *Cold Spring Harbor Perspect. Biol.* 10 (2018).
- [50] C.M. Giachelli, S. Steitz, Osteopontin: a versatile regulator of inflammation and biomineralization, *Matrix Biol.* 19 (2000) 615–622.
- [51] H. Arzate, M. Zeichner-David, G. Mercado-Celis, Cementum proteins: role in cementogenesis, biomineralization, periodontium formation and regeneration, *Periodontol.* 67 (2015) 211–233, 2000.
- [52] N. Laurens, P. Koolwijk, M.P.M. De Maat, Fibrin structure and wound healing, *J. Thromb. Haemostasis* 4 (2006) 932–939.
- [53] P.J. Marie, H. Miraoui, N. Severe, FGF/FGFR signaling in bone formation: progress and perspectives, *Growth Factors* 30 (2012) 117–123.
- [54] J.E. Chang, S.J. Turley, Stromal infrastructure of the lymph node and coordination of immunity, *Trends Immunol.* 36 (2015) 30–39.
- [55] R.E. Mebius, G. Kraal, Structure and function of the spleen, *Nat. Rev. Immunol.* 5 (2005) 606–616.
- [56] K.H. Mills, TLR-dependent T cell activation in autoimmunity, *Nat. Rev. Immunol.* 11 (2011) 807–822.
- [57] D.R. Harkness, Structure and function of immunoglobulins, *Postgrad. Med.* 48 (1970) 64–69.
- [58] S.R. Gonzales-van Horn, L.D. Estrada, N.S. van Oers, J.D. Farrar, STAT4-mediated transcriptional repression of the ILS gene in human memory Th2 cells, *Eur. J. Immunol.* 46 (2016) 1504–1510.
- [59] S.A. Oh, M.O. Li, TGF-beta: guardian of T cell function, *J. Immunol.* 191 (2013) 3973–3979.
- [60] S. Wormald, D.J. Hilton, Inhibitors of cytokine signal transduction, *J. Biol. Chem.* 279 (2004) 821–824.
- [61] X. Wang, L. Chung, J. Hooks, D.R. Maestas Jr., A. Lebid, J.I. Andorko, et al., Type 2 immunity induced by bladder extracellular matrix enhances corneal wound healing, *Sci. Adv.* (2021) 7.
- [62] D.S. Dzhaliolova, A.M. Kosyreva, M.E. Diatropov, N.A. Zolotova, I.S. Tsvetkov, V.A. Mkhitarov, et al., Morphological characteristics of the thymus and spleen and the subpopulation composition of lymphocytes in peripheral blood during systemic inflammatory response in male rats with different resistance to hypoxia, *Int. J. Inflamm.* 2019 (2019), 7584685.
- [63] R.E. Mebius, G. Kraal, Structure and function of the spleen, *Nat. Rev. Immunol.* 5 (2005) 606–616.
- [64] B.L. Foster, Methods for studying tooth root cementum by light microscopy, *Int. J. Oral Sci.* 4 (2012) 119–128.
- [65] W. Beertsen, C.A. McCulloch, J. Sodek, The periodontal ligament: a unique, multifunctional connective tissue, *Periodontol.* 13 (1997) 20–40, 2000.
- [66] K.M. Hotchkiss, N.M. Clark, R. Olivares-Navarrete, Macrophage response to hydrophilic biomaterials regulates MSC recruitment and T-helper cell populations, *Biomaterials* 182 (2018) 202–215.
- [67] D.R. Griffin, M.M. Archang, C.H. Kuan, W.M. Weaver, J.S. Weinstein, A.C. Feng, et al., Activating an adaptive immune response from a hydrogel scaffold imparts regenerative wound healing, *Nat. Mater.* 20 (2021) 560–569.
- [68] R. Liu, Y. Lin, J. Lin, L. Zhang, X. Mao, B. Huang, et al., Blood prefabrication subcutaneous small animal model for the evaluation of bone substitute materials, *ACS Biomater. Sci. Eng.* 4 (2018) 2516–2527.
- [69] Q. Liu, Z. Chen, H. Gu, Z. Chen, Preparation and characterization of fluorinated porcine hydroxyapatite, *Dent. Mater. J.* 31 (2012) 742–750.